Submitted to Journal of Alloys and Compounds as a regular article.

Self-propagating high-temperature synthesis of $LaMO_3$perovskite-type oxide using heteronuclearcyano metal complex precursors

Daniel Sánchez-Rodríguez,[1*] Hiroki Wada,[2] SyuheiYamaguchi,[2] Jordi Farjas,[1] and Hidenori Yahiro[2*]

[1]*GRMT, Department of Physics, University of Girona, Campus Montilivi, Edif.PII, E17071 Girona, Catalonia, Spain*

[2]*Department of Materials Science and Biotechnology, Graduate School of Science and Engineering, Ehime University, Matsuyama 790-8577, Japan*

*Corresponding authors:

yahiro.hidenori.me@ehime-u.ac.jp (H.Yahiro).

daniel.sanchez@udg.edu (D. Sánchez-Rodríguez).

Abstract

The decomposition of $La[Fe(CN)_6]$ and $La[Co(CN)_6]$ under different atmospheres has been analyzed by thermogravimetry (TG) and differential thermal analysis (DTA). In addition, the decomposition temperature at different sample locations was monitored for sample masses around 2 g of $La[Fe(CN)_6]$ and $La[Co(CN)_6]$, when they were calcined for 1 h at temperatures ranging from 200 to 400 ºC in a controlled gas-flow system. Results showed that, for sample large enough of these cyano complex precursors undergo combustion when are decomposed under oxygen atmosphere. X-ray diffraction

revealed that perovskite-type oxides crystallize due to the overheating of the process. As a result, it has been possible to produce $LaFeO_3$ and $LaCoO_3$ perovskite-type oxide powders by SHS under oxygen atmosphere using $La[Fe(CN)_6]$ and $La[Co(CN)_6]$ as a precursor. The effect of the ignition temperature has been investigated. The specific surface area of the perovskite-type oxides produced via SHS using heteronuclearcyano metal complex as a precursor is significantly higher than that of other $LaMO_3$ produced using the same technique but obtained from other type of precursors.
Keywords: combustion synthesis; SHS; heteronuclearcyano complex; *perovskite-type oxide*

1. Introduction

Perovskite-type oxide, ABO_3, has attracted much attention in the environmental-friendly catalytic systems. Up to date, the perovskite-type oxides have been reported to exhibit high catalytic activity for oxidations of hydrocarbon [1,2] and chlorinated volatile organic compounds [3], and decomposition of NO [4-6]. In addition, the perovskite-type oxides have been widely investigated to be employed as electrode materials [7-10] and sensing materials [11-21].

The preparation method of perovskite-type oxide catalyst has been progressively improved. Traditionally, perovskite-type oxides were prepared by solid state reaction of oxides and/or carbonates [22-24]. However, such a traditional method possesses the disadvantages of long processing time, low surface area, large particle size, and limited degree of chemical homogeneity. In 1967, Merzhanov et al. [25] reported the self-propagating high temperature synthesis (SHS) method which takes advantage of a combustion reaction in order to synthesize advanced materials. Most of the heat required for the synthesis is provided by the reaction itself. Therefore, its treatment

temperature and the processing time are significantly lower than those of conventional preparation routes. One can also expect to produce very fine and crystalline perovskite-type oxide powders by using this SHS method [26-28].Other combustion techniques are widely used to synthesize solid catalyst [29, 30]. Among them, the solution combustion synthesis (SCS) method is used to synthesize perovskite-type oxides [31]. In this technique, the liquid solution of a metal salt with a solvent as a fuel is heated until combustion occurs. Additionally, it is pertinent to remark that the SHS method differs substantially from the SCS method including the use of an ignition mechanism which heats locally the sample instead of heating the sample uniformly until volumetric combustion occurs [32].

The thermal decomposition of heteronuclearcyano metal complex (CN method) is also used to prepare perovskite-type oxides because of their similar structure. It was introduced in 1968 by Gallager but it must be emphasized the extensive study carried out by Sadaoka and co-workers in the 1990s [19, 33-39]. In these papers, the preparation of perovskite-type oxides $LaFeO_3$ and $LaCoO_3$ from coordination polymer precursors, $La[Fe(CN)_6]\cdot 5H_2O$, and $La[Co(CN)_6]\cdot 5H_2O$ calcined in a gas-flow system at several conditions, such as temperature, time, and atmosphere, has been investigated. These studies revealed that under oxygen atmosphere, both precursors decompose by a combustion process in which a solid-state self-sustained reaction transforms progressively the sample into the desired perovskite-type oxide. Reaction is not homogenous over the sample but it is confined in a combustion front. This result opens the door to the decomposition of heteronuclearcyano metal complex for the synthesis of perovskite-type oxides via SHS.

In this paper we analyze the synthesis of $LaFeO_3$and $LaCoO_3$perovskite-typeoxides via SHS using heteronuclearcyano metal complex as a precursor. Results will be

compared with those of similar perovskite-type oxides obtained via SHS using a mixture of different powders as a precursor [26,27].

2. Experimental details

Commercial compounds, $La(NO_3)_3 \cdot 6H_2O$ (Wako, 99.5%), $K_3[Fe(CN)_6]$(Hayashi, 99%) and $K_3[Co(CN)_6]$(Sigma-Aldrich, 99%),were used without further purification. $La[Fe(CN)_6] \cdot 5H_2O$ as a precursor of perovskite-type oxide, $LaFeO_3$,was precipitated immediately after mixing 1 M aqueous solutions of $La(NO_3)_3 \cdot 6H_2O$ and $K_3Fe(CN)_6$at room temperature under continuous stirring. By a similar way, $La[Co(CN)_6] \cdot 5H_2O$ precursor was obtained from $La(NO_3)_3 \cdot 6H_2O$ and $K_3Co(CN)_6$1 M mixed solutions. According to the method previously reported by Traversa et al.[37], the resulting precipitates were collected by suction filtration, washed with deionized water, ethanol and diethyl ether, and then finally dried in air at 50ºC.

For systematic analysis, cyano complex precursors were calcined for 1 h at several treatment temperatures ranging from 200 to 400 ºC in a gas-flow system using an electric furnace and alumina pipe (Fig. 1a); the samples were exposed to several gas atmospheres such as oxygen, air and nitrogen atmospheres. The flow rate of each gas was set at 50 $mL \cdot min^{-1}$.

Perovskite-type oxides were obtained by SHS after preheating the prepared cyano complex precursor at several treatment temperatures from room temperature up to 150 ºC using the same gas-flow system. The schematic view of the system is depicted in Fig.1b. A nichrome wire connected to a voltage slider was placed on the top of one of the extremes of the samples as combustion ignitor. After the samples were heated to desired temperature, a voltage of 10 V was applied to the ignitor for several seconds until a combustion front was set. In this experiments, oxygen was introduced with 50

$mL \cdot min^{-1}$ of gas flow rate.

Thermogravimetric (TG) and differential thermal analysis (DTA) experiments were performed simultaneously with a Shimadzu DTG-60E. Powder XRD patterns were obtained by a RigakuMiniFlex II diffractometer using CuK α radiation. BET analysis (Belsorp-mini, BEL JAPAN) was performed to determine the specific surface area by measuring the adsorption-desorption capacity using N_2 adsorbent at -196ºC.

3. Results and discussion

3.1 Thermal analysis of the decomposition of$La[Fe(CN)_6]$ and $La[Co(CN)_6]$

Figures 2 and 3 show TG curves of $La[Fe(CN)_6]$ and $La[Co(CN)_6]$ with different sample masses, respectively. These TG experiments were carried out in flowing oxygen (a), air (b), and nitrogen (c). The decomposition process of $La[Fe(CN)_6]$ and $La[Co(CN)_6]$ was faster when the sample mass was increased under oxidant atmosphere (see Figure 2(a, b) and Figure 3(a, b), respectively). Later on it is shown that this behavior is associated to a sample overheating due to an exothermic reaction for oxidation of cyano groups in samples. A similar behavior has been reported before in the decompositions of other metalorganic powders [40, 41]. In the particular case of pure oxygen atmosphere, the extremely abrupt decomposition curve associated with higher sample masses is due to the sample local overheating leads to a thermal runaway, as it will be shown in the following.

In the presence of oxygen, all $La[Co(CN)_6]$ samples but with the lowest mass (0.72 mg) exhibit the abrupt mass loss characteristic of the occurrence of a thermal runaway. This behavior is related to the fact that the critical mass for combustion is lower in the case of $La[Co(CN)_6]$ and it is too small to be accurately analyzed with our TG. Besides,

although the reaction is also exothermic under nitrogen atmosphere, no overheating is possible because heat removal through diffusion prevails over the heat evolved from the reaction. By increasing the thickness of sample powder, heat removal is slowed down. Theoretically [42]there is a critical mass above which thermal explosion is possible even in the case of nitrogen atmosphere. Notice that in the occurrence of a thermal runaway, the decomposition of $La[Fe(CN)_6]$ and $La[Co(CN)_6]$ is completed at 350ºC and 400ºC respectively. Conversely, in the absence of a thermal runaway, the decomposition is completed around 650ºC. This temperature coincides with the decomposition temperature of lanthanum dioxycarbonate (LaO_2CO_3) [43], an intermediate compound that has been detected by XRD (see in the following). In the occurrence of a thermal runaway, the reaction is self-accelerated and evolves very fast resulting in the very abrupt mass loss exhibit by the TG. Under this conditions the reaction proceeds quasi-adiabatically, i.e., locally the sample temperature may approach the adiabatic temperature [40, 44, 45] while the temperature at the crucible walls remains nearly unaltered. Therefore, the actual sample temperature may easily be few hundred degrees above the temperature recorded by the TG.

To proof it, significantly larger samples of $La[Fe(CN)_6]$ and $La[Co(CN)_6]$ precursors (~ 2 g) were treated during 1h in a gas-flow system composed by an electric furnace and alumina tube under several atmospheres and treatment temperatures (See Table 1). The evolution of the temperature during the most characteristic thermal treatments at different locations of the samples has been plotted for $La[Fe(CN)_6]$ and for $La[Co(CN)_6]$ in Figure 4 and Figure 5, respectively. When the furnace temperature is high enough, *i.e.*, 250ºC for $La[Fe(CN)_6]$ and 350ºC for $La[Co(CN)_6]$, a local overheating is clearly observed for both, oxygen and air atmospheres, although, it is significantly larger in the case of oxygen. Even so, TG curves showed that under air

atmosphere reaction is slightly delayed (Figure 2and Figure 3) with respect to oxygen. Therefore, we have plotted the temperature at different locations of a sample decomposed under air atmosphere for a treatment temperature 50ºC higher, *i.e.* 300 ºC for $La[Fe(CN)_6]$ and 400ºC for $La[Co(CN)_6]$.We have observed no significant difference under these temperatures with respect to experiments performed at 50ºC less. While under air atmosphere the overheating is of the order of tens of degree, under oxygen thermocouples register a rise of hundreds. As expected, when nitrogen was used as the surrounding gas, the sample temperature closely followed the furnace temperature during the whole treatment. In addition, under oxygen atmosphere, we observed a local overheating that propagates through the sample, *i.e.*, a combustion front is set. Moreover, if the furnace power is turned off when the thermal runaway starts, the reaction is self-sustained, i.e., further heating is not necessary for the reaction to progress (Figure 4c and Figure 5c). Therefore, one can assume that $La[Fe(CN)_6]$ and $La[Co(CN)_6]$ under oxygen atmosphere decompose via combustion provided that the sample is large enough. The minimum thickness above which these precursors decompose via combustion process is determined by several experimental settings such as the sample geometry, the thermal conductivity or the ignition mode. Thus, critical thickness of the experiments carried out in the gas flow system cannot be directly extrapolated from the TG curves. The whole decomposition process of both heteronuclearcyano complex precursors lasted about 20 min. Taking into account that the sample was5 cm long, it means that the front propagates at a velocity of 2.5 $mm \cdot min^{-1}$, which is an extremely slow speed for a combustion process [46].

The XRD patterns related to the experiments listed in Table 1 are plotted in Figure 6 and Figure 7. It can be noted that only in those experiments that undergo a combustion process the desired perovskite oxide crystallizes. XRD patterns b and c of Figure 7

reveals the presence of carbonates and/or nitrates derived from oxidation of cyano group when $La[Co(CN)_6]$ is decomposed at 350ºC, i.e. under volumetric combustion. Therefore, combustion does not guarantee the complete removal of carbon and/or nitrogen. We have identified (Figure 7) the presence of $La_2O_2CO_3$ and Co_3O_4. As we have mentioned before, the 3.4 mg mass sample treated under oxygen atmosphere (Figure 3a) undergoes a mass lost during decomposition that corresponds with the expected one if reaction product is pure $LaCoO_3$. This means that in TG experiments neither carbonatenor nitrate species are formed. This contradiction between small and large sample masses could be explained by the assumption that by increasing the sample thickness, the oxygen diffusion through the sample is reduced. This makes more difficult to remove the carbon and the nitrogen of the precursor. Then, it is logical to expect that the amounts of carbonates and nitrates could be controlled by controlling the oxygen diffusion. As the other possibility, the amounts of carbonates and nitrates may be affected by the thickness, particle size or gas flux rate. Under nitrogen atmosphere, $La[Fe(CN)_6]$and $La[Co(CN)_6]$ precursors are not completely decomposed even at 300 and 400ºC, respectively. Under air, $LaCoO_3$ starts to crystallize at 400ºC. However, sample temperature is too low so that it would be necessary to make the treatment duration significantly longer to achieve a product as crystalline as the obtained under oxygen atmosphere at 350ºC.

3.2 Production of $LaFeO_3$ and $LaCoO_3$perovskite-type oxides via. SHS

In view of the previous results, the possibility of producing $LaMO_3$ perovskite oxides by SHS has been considered. In this section, we report the effect of preheating the sample up to a specific temperature before the combustion front is set by ignition.

In Figure 8 and Figure 9, XRD patterns of $La[Fe(CN)_6]$ and $La[Co(CN)_6]$

decomposed by solid state combustion via electric ignition are shown. It can be seen that perovskite-type oxides are formed even at room temperature. In addition, it should be noted in Figure 9 that the XRD peaks corresponding to $La_2O_2CO_3$ were observed after the combustion of $La[Co(CN)_6]$, although the amount of carbonate seems to decrease when the sample is preheated at higher temperatures. A low intensity peak appears at 18.7º in the $La[Fe(CN)_6]$ sample preheated at 50ºC and in the $La[Fe(CN)_6]$ sample preheated at 100ºC, Indicating that in some cases the small amounts of precursor left unreacted. The high concentration of defects such as unreacted precursor or intermediate compounds is characteristic of this technique and usually improves the catalytic activity of the final product by increasing the specific surface area. Figure 10 shows the photographs of $La[Fe(CN)_6]$ and $La[Co(CN)_6]$ samples and their corresponding perovskite-type oxides produced after the SHS treatment. It is clearly observed that those samples are not homogeneous. The product obtained by the decomposition of $La[Fe(CN)_6]$ presents different shades with brown color. Although the product of decomposing $La[Co(CN)_6]$ is all black, some white unreacted precursors remain in the vicinity of the supporting glass tube. It is important to emphasize that these precursors do not decompose by an explosive reaction but by a slow combustion process. This is particularly suited to the synthesis of films because all the reacted sample remains on the support. Independently of the preheating temperature, particle morphology and size are very similar as shown in the scanning electrons micrographs (SEM) of Figure 11 and Figure 12.The intensity peaks of X-ray diffraction appear to be higher when the sample is preheated at a higher temperature.

The specific surface areas (SSA) of the previous samples are summarized in Table 2. The SSA of $LaFeO_3$ produced by the decomposition of $La[Fe(CN)_6]$via solid state combustion decreased with increasing preheating temperature: 29.6 $m^2 \cdot g^{-1}$ at 50ºC of

preheating temperature and 17.2 $m^2 \cdot g^{-1}$at 150ºC. The $LaCoO_3$ counterparts range from 12.3to 8.4$m^2 \cdot g^{-1}$. These values are much higher than those expected from the size of the particles showed in Figures 11 and 12. However, an explanation for such a high surface areas could be provided by magnification of the SEM images. In Figure 13 we can observe porous in the $LaCoO_3$ particles and cracks in $LaFeO_3$ particles. In addition, it could be expected that the combustion front temperature will increase by increasing the preheating furnace temperature. Consequently the crystallinity of the sample will also increase. However, there is a low correlation between SSA and the ignition temperature. This is probably related to the variations in the combustion front temperature while crossing the sample (Figure 4c and Figure 5c). Therefore, it is difficult to obtain a homogeneous product (Figure 10). However, it is significant that the SSAs of $LaFeO_3$ and $LaCoO_3$ synthesized by SHS using heteronuclearcyano complex precursors are much larger than those of $LaMO_3$ perovskite oxides synthesized by SHS using a mixture of powders: $La_{1-x}Sr_xMnO_3$ from La_2O_3, $SrCO_3$, Mn and $NaClO_4$ (0.116-0758 m^2/g) [26] and $La_{1-x}Sr_xFeO_3$ from La_2O_3, $SrCO_3$, Fe and $NaClO_4$ (0.1-2.2 m^2/g) [27].

4. Conclusions

(1) $La[Fe(CN)_6]$ and $La[Co(CN)_6]$ decompose via a combustion process under oxygen atmosphere when sample is large enough. This fact allows the synthesis of perovskite-type oxides at temperatures that otherwise would be significantly higher.

(2) $LaFeO_3$ and $LaCoO_3$perovskite-type oxide were successfully produced by the SHS method even at room temperature. However, we have not been able to obtain carbon free $LaCoO_3$even if the cyano complex precursor is preheated up to 150ºC.

(3) The specific surface area of $LaFeO_3$and $LaCoO_3$perovskite-typeoxides produced via

SHS using heteronuclearcyano metal complex as precursors was higher than that of $LaMO_3$ obtained with the same technique but using other precursors.

Acknowledgements

This work was partially funded by the KAKENHI Grant Number 24560948. D. S.-R. thanks the University of Girona and the NESSIE program for the PhD fellowships.

References

[1] Johnson, D. W., Jr., Gallagher, P. K., Wertheim, G. K. and Vogel, E. M., *J. Catal.*, **48** (1977) 87-97.

[2] Yasuda, H., Fujiwara, Y., Mizuno, N. and Misono, M.,*J. Chem. Soc., Faraday Trans.*, **90** (1994) 1183-1189.

[3] Barbero, B. P., Gamboa, J. A. and Cadús, L. E., *Appl. Catal. B*, **65** (2006) 21-30.

[4] Teraoka, Y., Fukuda, H. and Kagawa, S., *Chem. Lett.*, **19** (1990) 1-4.

[5] Teraoka, Y., Nakano, K., Shangguan, W. and Kagawa, S., *Catal. Today*, **27** (1996) 107-113.

[6] Dai, H., He, H., Li, P, Gao, L. and Au, C.-T., *Catal. Today*, **90** (2004) 231-244.

[7] Minh, N. Q., *J. Am. Ceram. Soc.*, **76** (1993) 563-588.

[8] Inoue, T., Seki, N., Eguchi, K. and Arai, H., *J. Electrochem. Soc.*, **137** (1990) 2523-2527.

[9] Alcock, C. B., Doshi, R. C. and Shen, Y., *Solid State Ionics*, **51** (1992) 281-289.

[10] Shuk, P., Vecher, A., Kharton, V., Tichonova, L., Wiemhöfer, H. D., Guth, U. and Göpel, W., *Sens. Actuators B*, **16** (1993) 401-405.

[11] Shimizu, Y., Shimabukuro, M., Arai, H. and Seiyama, T., *Chem. Lett.* **14** (1985) 917-920.

[12] Lukaszewicz, J. P., *Sens. Actuators B*, **4** (1991) 227-232.

[13] Obayashi, H. and Kudo, T., *Nippon Kagaku Kaishi* (1980) 1568-1572.

[14] Yu, C., Shimizu, Y. and Arai, H., *Chem. Lett.* **15** (1986) 563-566.

[15] Post, M. L., Sanders, B. W. and Kennepohl, P., *Sens. Actuators B*, **13** (1993) 272-275.

[16] Li, W. B., Yoneyama, H. and Tamura, H., *Nippon Kagaku Kaishi* (1982) 761-767.

[17] Takahashi, Y. and Taguchi, H., *J. Mater. Sci. Lett.*, **3** (1984) 251-252.

[18] Arakawa, T., Takada, K., Tsunemine, Y. and Shiokawa, J., *Sens. Actuators*, **14** (1988) 215-221.

[19] Matsuura, Y., Matsushima, S., Sakamoto, M. and Sadaoka, Y., *J. Mater. Chem.*, **3** (1993) 767-769.

[20] Traversa, E., Matsushima, S., Okada, G., Sadaoka, Y., Sakai, Y. and Watanabe, K., *Sens. Actuators B*, **25** (1995) 661-664.

[21] Arakawa, T., Kurachi, H. and Shiokawa, J., *J. Mater. Sci.*, **20** (1985) 1207-1210.

[22] Royer, S., Bérubé, F. and Kaliaguine, S., *Appl. Catal. A*, **282** (2005) 273-284.

[23] Bell, R. J., Millar, G. J. and Drennan, J., *Solid State Ionics*, **131** (2000) 211-220.

[24] Rida, K., Benabbas, A., Bouremmad, F., Peña, M. A. and Martínez-Arias, A., *Catal. Commun.*, **7** (2006) 963-968.

[25] Merzhanov, A. G., *Ceramics International*, **21** (1995) 371-379.

[26] Hirano, T., Purwanto, H., Watanabe, T.,andAkiyama, T., *J. AlloysCompd*, **441** (2007) 263-266.

[27] Hirano, T., Tosho, T., Watanabe, T., Akiyama, T., *J. AlloysCompd*, **470** (2009) 245-249.

[28] Ming, Q., Nerseyan, N. D., Richardson, J. T., and Luss, D., *J Mater. Sci.*, **35** (2000) 3599-3606.

[29] Patil, K. C., Aruna, S. T., and Mimani, T.,*Curr. Opin.Solid State Mater. Sci.*, **6** (2002) 507-512

[30] Zhu, C., Nobuta, A., Nakatsugawa, I., and Akiyama, T., *Int. J. Hydrogen Energy*, **38** (2013) 13238-13248

[31] Civera, A., Pavese, M., Saracco, G., andSpecchia, V.,*Catal. Today*, **83** (2003) 199-211.

[32] González-Cortés, L. S. andImbert, F. E., *Appl. Catal. A*, **452** (2013) 117-131.

[33] Sadaoka, Y., Traversa, E., and Sakamoto, M., *Chem. Lett.*, **25** (1996) 177-178.

[34] Sadaoka, Y., Traversa, E., and Sakamoto, M., *J. Alloys Compd.*, **240** (1996) 51-59.

[35] Sakamoto, M., Nunziante, P., Traversa, E., Matsushima, S., Miwa, M., Aono, H., and Sadaoka, Y., *J. Ceram. Soc. Jpn.*, **105** (1997) 693-696.

[36] Traversa, E., Nunziante, P., Sakamoto, M., Sadaoka, Y., Carotta, M. C., and Martinelli, G., *J. Mater. Res.*, **13** (1998) 1335-1344.

[37] Traversa, E., Nunziante, P., Sakamoto, M., Sadaoka, Y., and Montanari, R., *Mater. Res. Bull.*, **33** (1998) 673-681.

[38] Sadaoka, Y., Aono, H., Traversa, E., and Sakamoto, M., *J. AlloysCompd.*, **278** (1998) 135-141.

[39] Aono, H., Sato, M., Traversa, E., Sakamoto, M., and Sadaoka, Y., *J. Am. Ceram. Soc.*, **84** (2001) 341-347.

[40] Sánchez-Rodríguez, D., Eloussifi, H., Farjas, J., Roura, P., and Dammak, M., *Thermochim. Acta*,**589** (2014) 37–46.

[41] Sanchez-Rodriguez, D., Farjas, J., Roura, P., Ricart, S., Mestres, N., Obradors, X., and Puig, T., *J. Phys.Chem. C*, **117** (2013) 20133–20138.

[42] Frank-Kamenetskii, *Diffusion and Heat Exchange in Chemical Kinetics*, Princeton University Press, New Jersey, 1955.

[43] Shirsat, A.N., Ali M.,Kaimal, K.N.G., Bharadwaj, S.R. and Das, D.,*Thermochim. Acta*,**399** (2003) 167–170.

[44] Boddington, T., Hongtu, F., Laye, P.G., Nawaz, M., Nelson, D.C., *Thermochim. Acta* **170** (1990) 81–87.

[45] Morsi, K., *J. Mater. Sci.* **47** (2011) 68–92.

[46] Yeh, C.-L., *Encycl. Mater. Sci. Technol.* (2010) 1–8.

Table 1. Experiments performed with the gas flow system.

Precursor	**Atmosphere**	**Treatment temperature (**^{o}C)	**Treatment duration (h)**
$La[Fe(CN)_6]$	O_2	200	1
$La[Fe(CN)_6]$	O_2	250	1
$La[Fe(CN)_6]$	O_2	250	Furnace power off once combustion starts
$La[Fe(CN)_6]$	Air	250	1
$La[Fe(CN)_6]$	Air	300	1
$La[Fe(CN)_6]$	N_2	250	1
$La[Fe(CN)_6]$	N_2	300	1
$La[Co(CN)_6]$	O_2	300	1
$La[Co(CN)_6]$	O_2	350	1
$La[Co(CN)_6]$	O_2	350	Furnace power of once combustion starts
$La[Co(CN)_6]$	Air	350	1
$La[Co(CN)_6]$	Air	400	1
$La[Co(CN)_6]$	N_2	350	1
$La[Co(CN)_6]$	N_2	400	1

Table 2.Specific surface area of perovskite-type oxides obtained by SHS

Precursor	Ignition temperature (ºC)	SSA ($m^2 \cdot g^{-1}$)
$La[Fe(CN)_6]$	Room temperature	17.8
$La[Fe(CN)_6]$	50	29.6
$La[Fe(CN)_6]$	100	28.6
$La[Fe(CN)_6]$	150	17.2
$La[Co(CN)_6]$	Room temperature	11.3
$La[Co(CN)_6]$	50	10.2
$La[Co(CN)_6]$	100	12.3
$La[Co(CN)_6]$	150	8.4

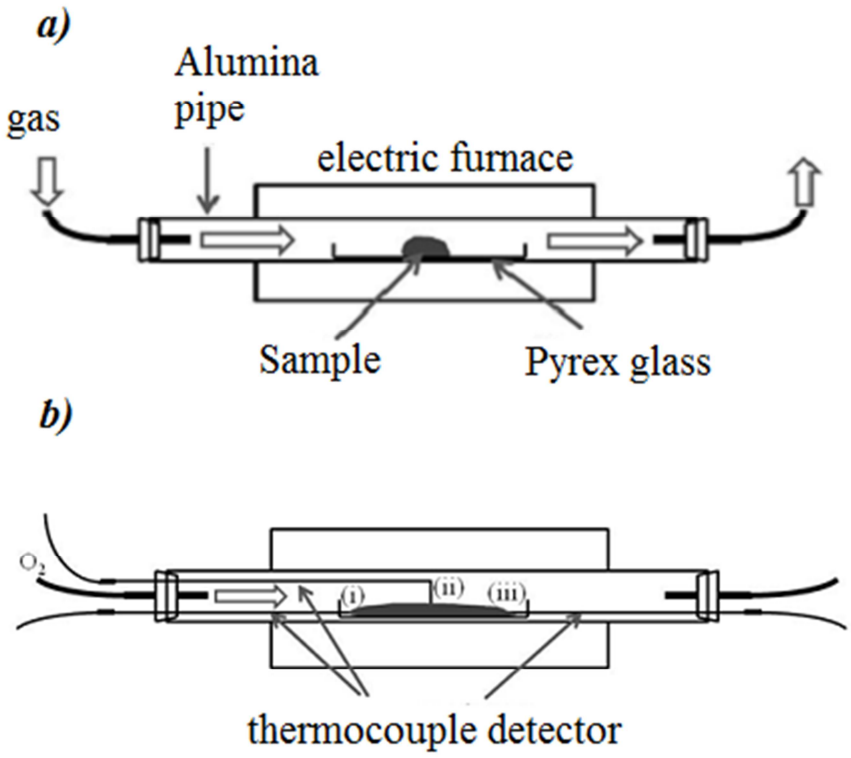

Figure 1. The apparatus of gas-flow system (a) and the locations of thermocouple detectors at on the sample, such as entrance (i), middle (ii), and exit sites(iii) (b).

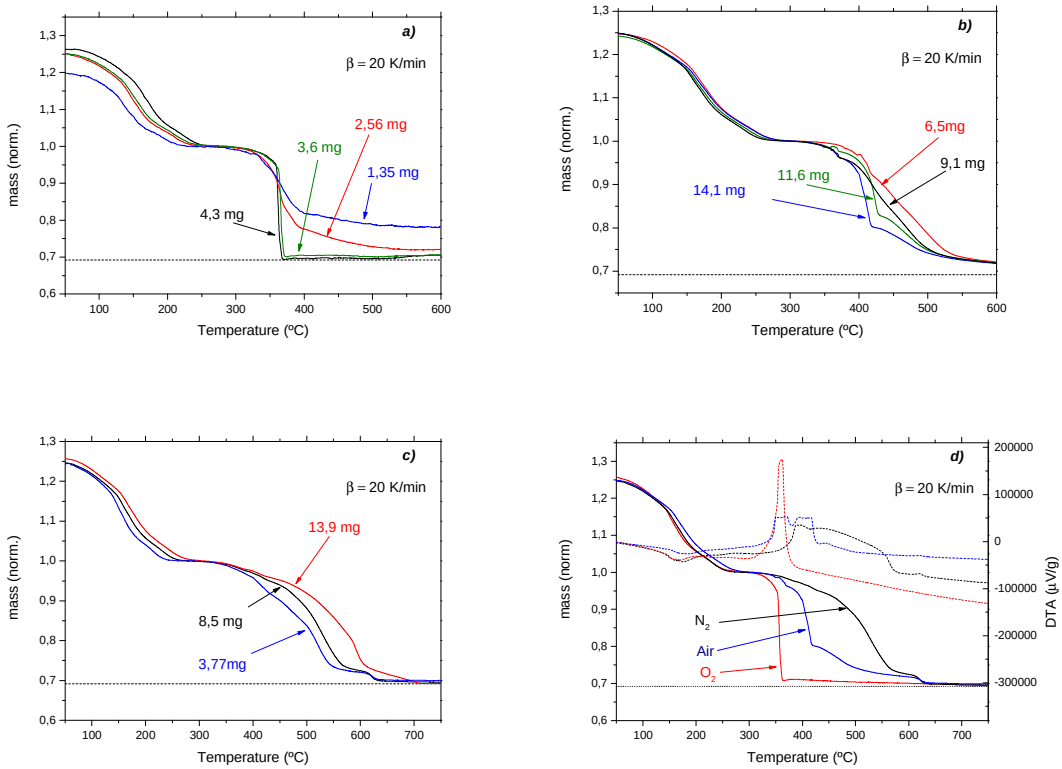

Figure 2. Evolution of the thermal decomposition of $La[Fe(CN)_6]$under O_2 (a), air (b) and N_2 (c) for different sample masses. Plot (d) shows a comparison of the characteristic thermal decomposition for high sample masses under different atmospheres. Horizontal dotted line indicates the mass of pure $LaFeO_3$.

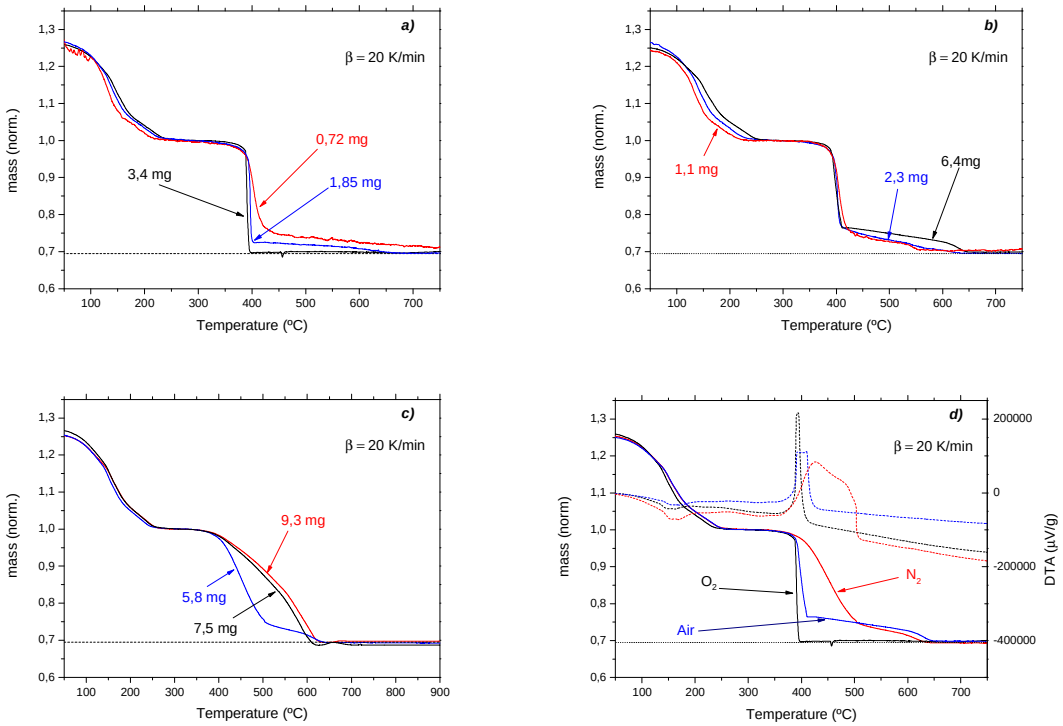

Figure 3.Evolution of the thermal decomposition of $La[Co(CN)_6]$ under O_2 (a), air (b) and N_2 (c) for different sample masses. Plot (d) shows a comparison of the characteristic thermal decomposition for high sample masses under different atmospheres including DTA measurement. Horizontal dotted line indicates the mass of pure $LaCoO_3$.

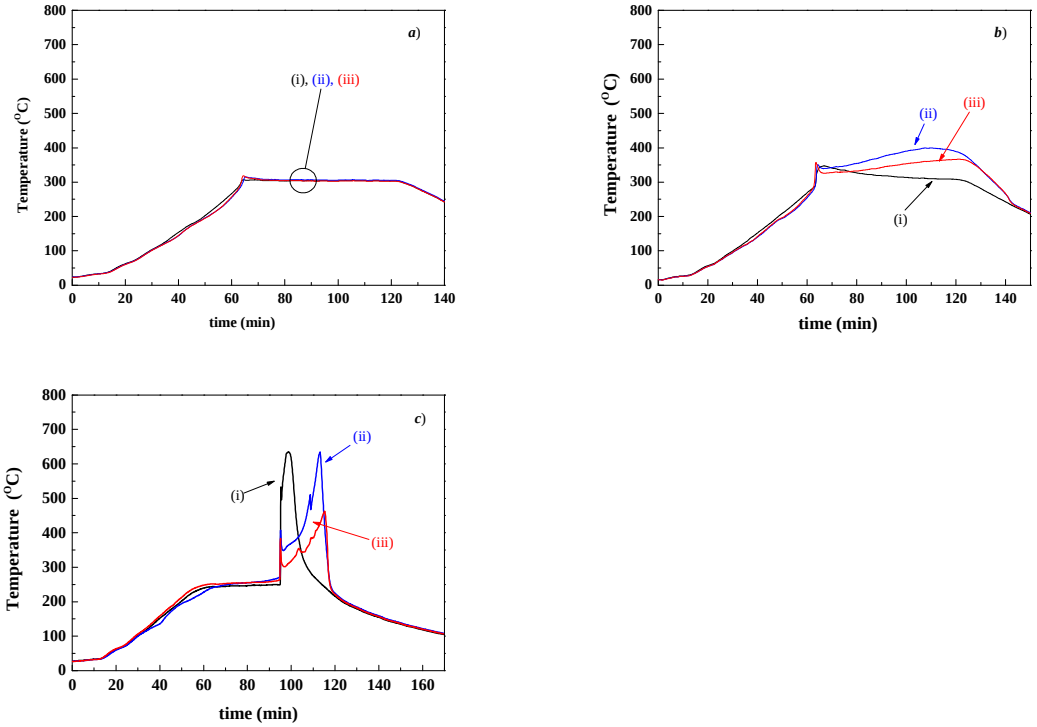

Figure 4.Evolution of the temperature at different positions of the sample: the extreme closer to the gas entrance(i), in the middle (ii) and at the extreme opposite to the gas entrance(iii). La[Fe(CN)$_6$] treated under different atmospheres and during different times: (a) N_2-300°C-1h , (b) Air-300°C-1h (c) O_2-250°C. The furnace is powered off after combustion starts (approximately 40min. at 250°C).

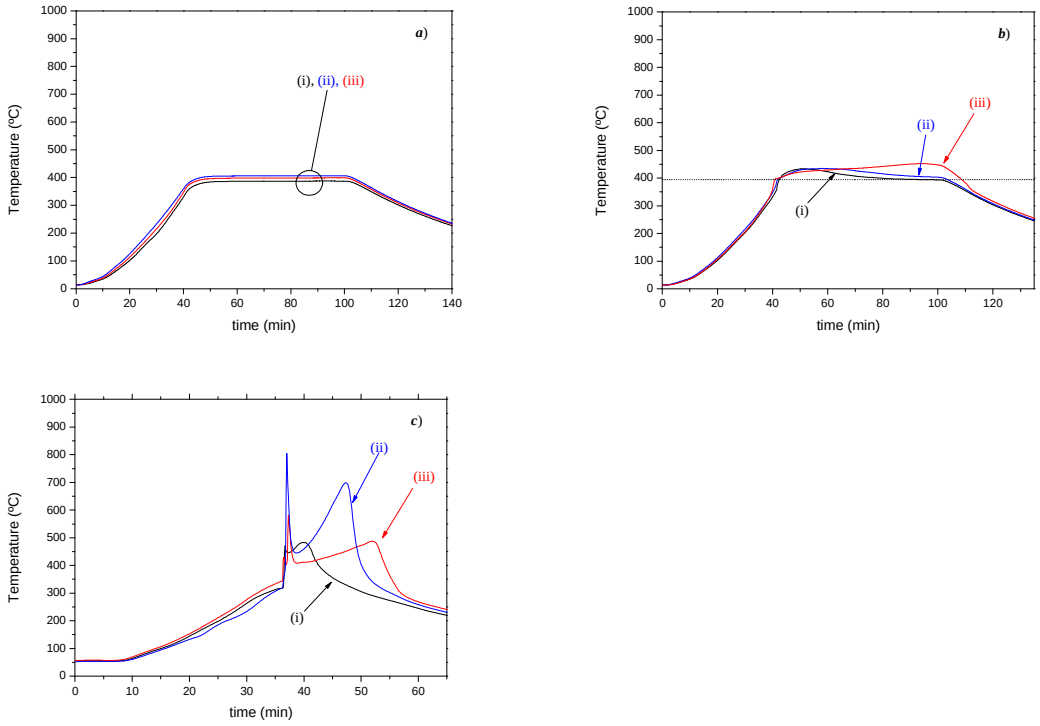

Figure 5. Evolution of the temperature at different positions of the sample: the extreme closer to the gas entrance (i), in the middle (ii) and at the extreme opposite to the gas entrance(iii). La[Co(CN)$_6$] treated under different atmospheres and during different times: (a) N_2-400ºC-1h , (b) Air-400ºC-1h, (c) O_2-350ºC. Thefurnace is powered off after combustion starts (approximately 2 min. at 350ºC).

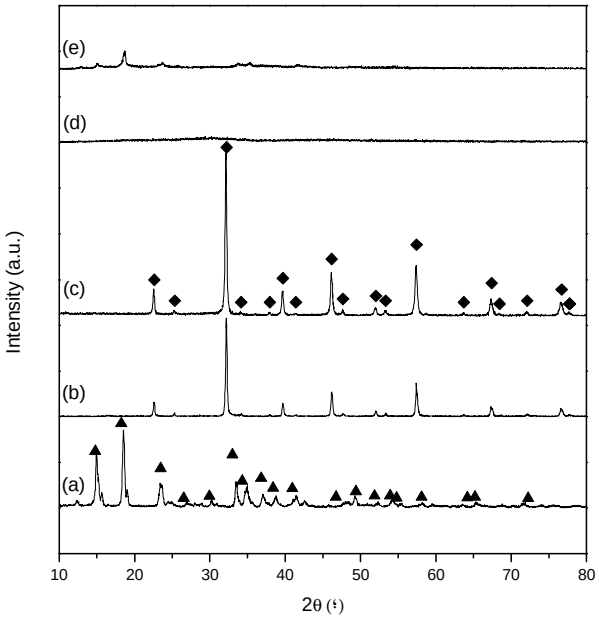

Figure 6.XRD patterns of $La[Fe(CN)_6]\cdot 5H_2O$treated under different atmospheres and during different times: (a) O_2-200ºC-1h , (b) O_2-250ºC-1h (c) O_2-250ºC-Furnace powered off once combustion starts (approximately 40 min at 250ºC), (d) N_2-300ºC-1h,(e) Air-300ºC-1h.♦: $LaFeO_3$, ▲: $La[Fe(CN)_6]$.

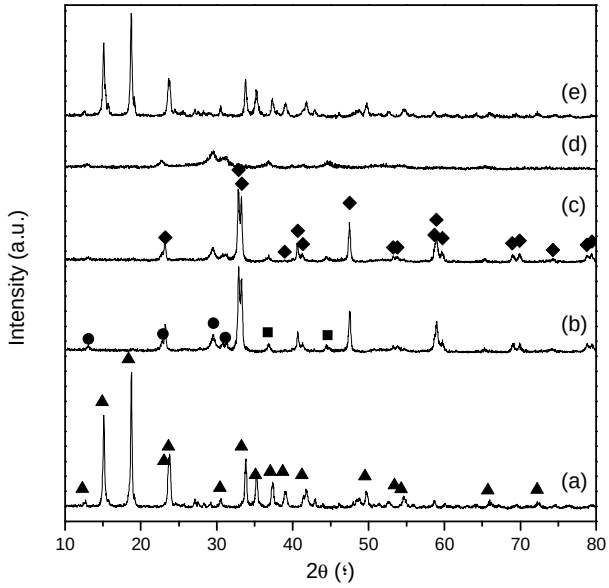

Figure 7. XRD patterns of $La[Co(CN)_6]\cdot 5H_2O$treated under different atmospheres and during different times: (a) O_2-300ºC-1h , (b) O_2-350ºC-1h (c) O_2-350ºC-Furnace powered off once combustion starts (approximately 2 min. at 350ºC), (d) N_2-400ºC-1h,(e) Air-400ºC-1h.♦:$LaCoO_3$, ●: $La_2O_2CO_3$, ▲: $La[Co(CN)_6]$, ■:Co_3O_4.

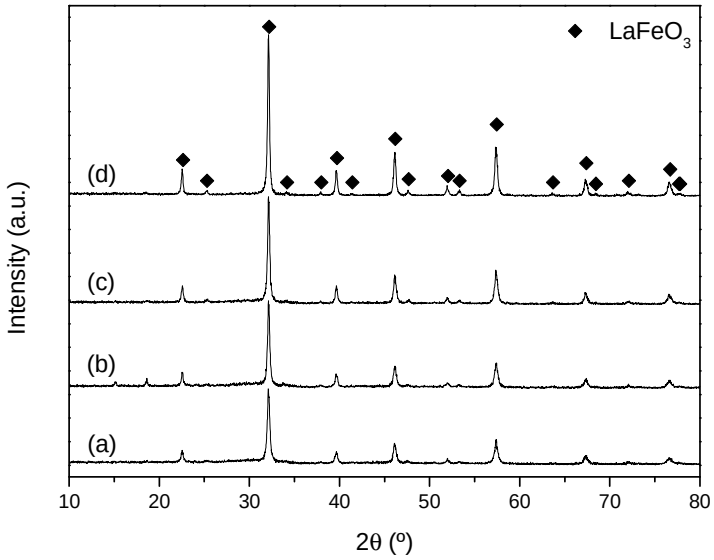

Figure 8. XRD patterns of $LaFeO_3$ produced by SHS. Electric ignition at room temperature (a), 50°C (b), 100°C(c), and 150°C (d). ♦:$LaFeO_3$.

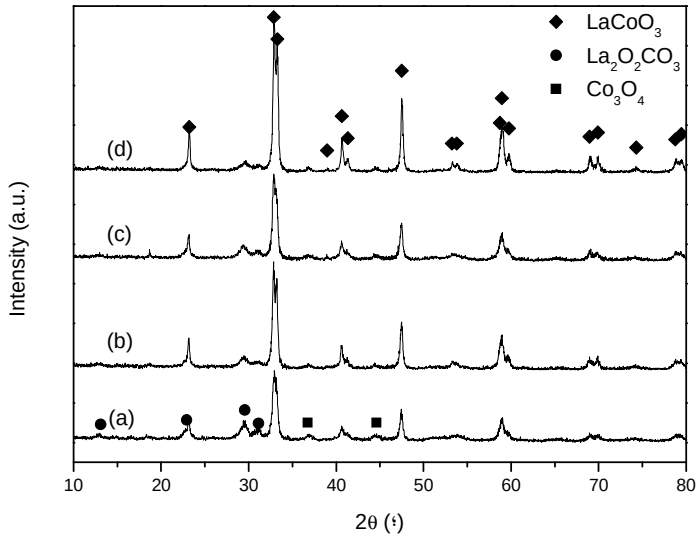

Figure 9.XRD patterns of $LaCoO_3$ produced by SHS. Electric ignition at room temperature (a), 50°C (b), 100°C(c), and 150°C (d).●: $La_2O_2CO_3$, ♦:$LaCoO_3$, ■:Co_3O_4..

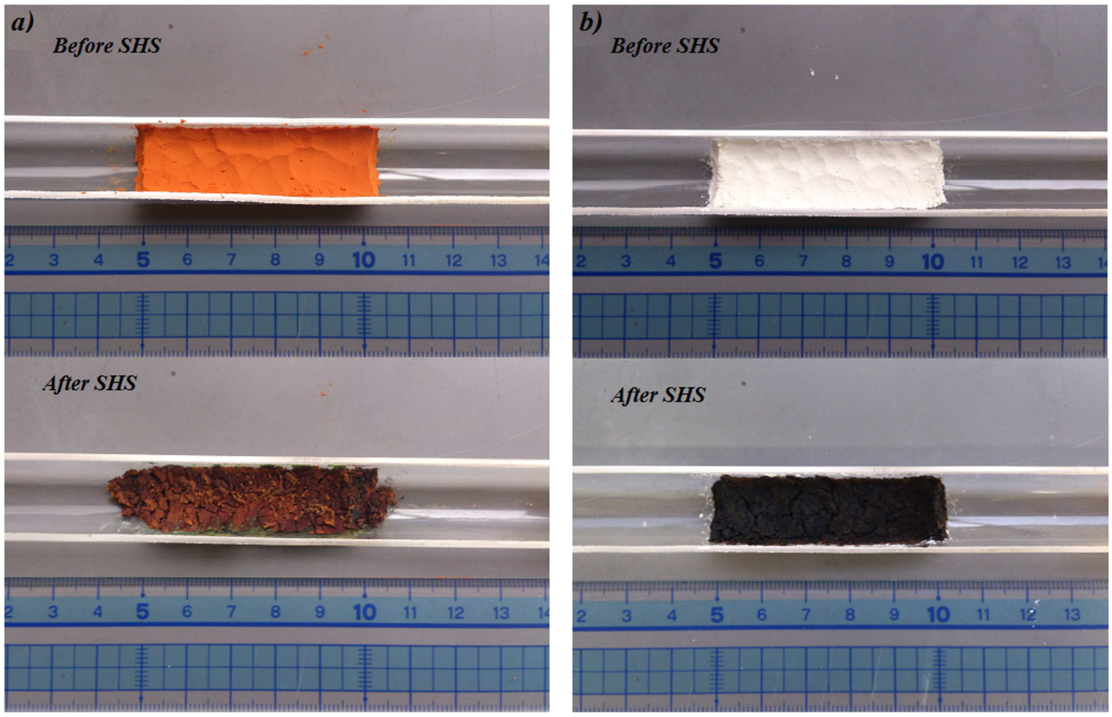

Figure 10 Photographs of $LaFeO_3$ (a) and $LaCoO_3$ (b)samples and its respectively perovskite-type oxides produced by SHS.

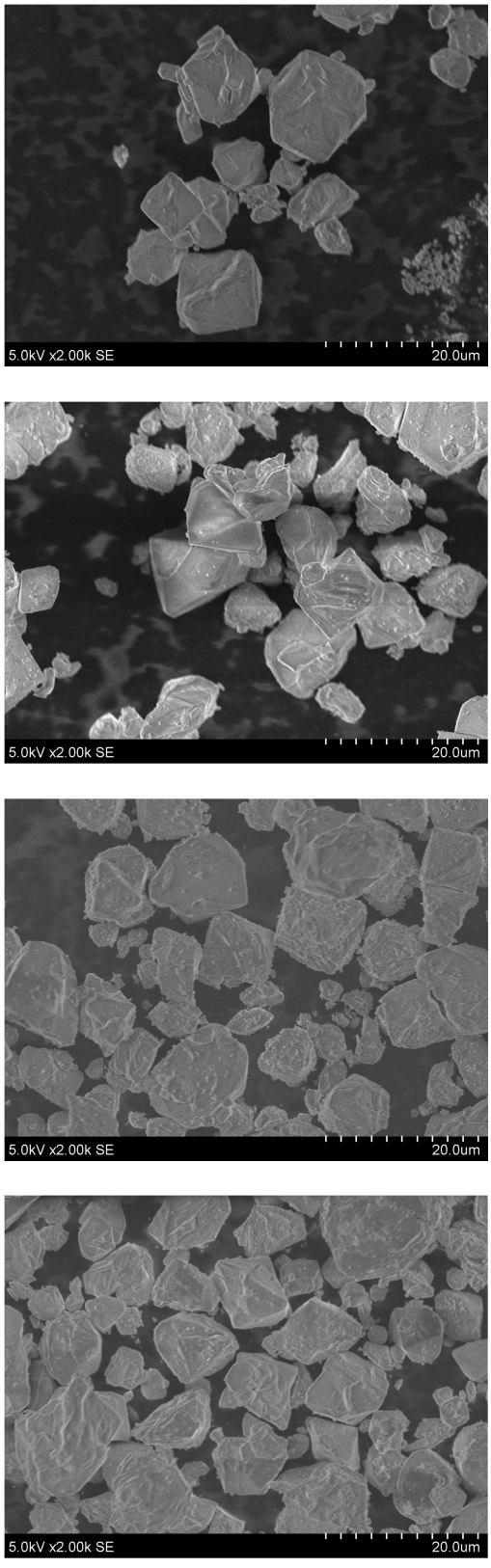

Figure 11.*From top to bottom*: SEM micrographs of $LaFeO_3$ produced by SHS at an ignition temperature of 150°C, 100°C, 50°C, and room temperature.

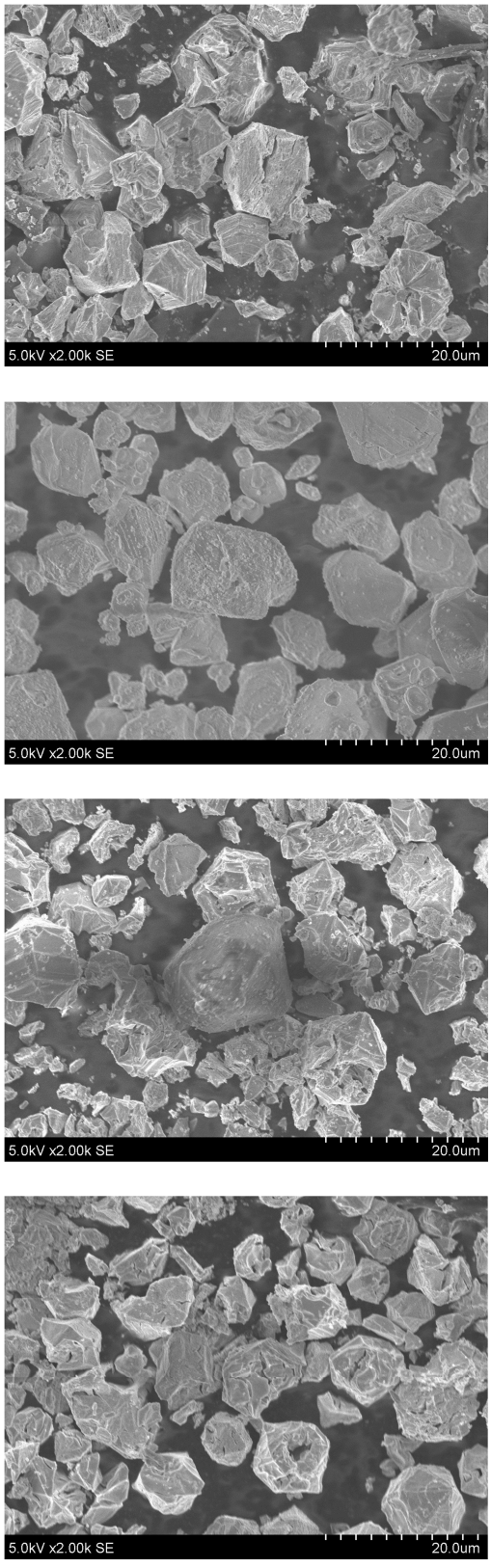

Figure 12. ***From top to bottom*****: SEM micrographs of $LaCoO_3$ produced by SHS at an ignition temperature of 150°C, 100°C, 50°C, and room temperature.**

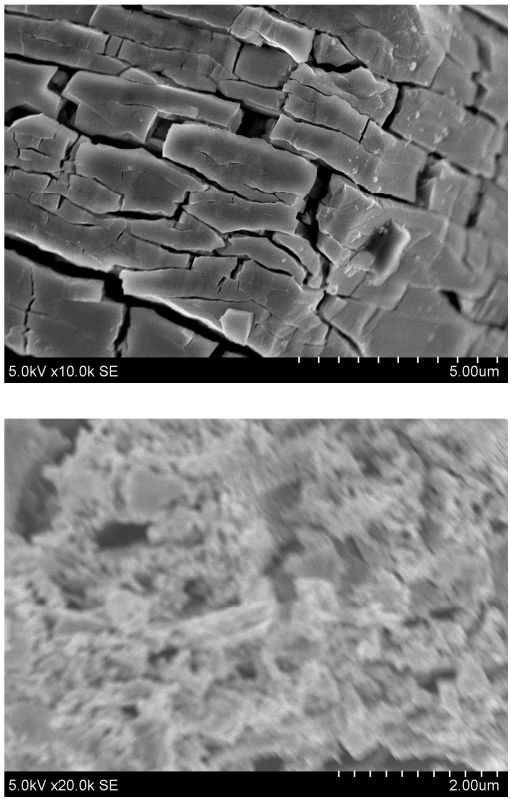

Figure 13. Characteristic SEM micrographs of the LaFeO3 (top) and LaCoO3 (bottom) powder surfaces produced by SHS.